Stochastic resetting and hierarchical synchronization

Meylahn, J.M.

CHAPTER 1
Introduction

This thesis consists of two parts. Part I focusses on large deviations of stochastic processes with resetting, Part II focusses on the Kuramoto model on networks with community structure.

Part I

Stochastic resetting is simple enough to be approached analytically, yet modifies stochastic processes in a non-trivial way. It has recently received renewed attention in the mathematical physics literature. In part I of the thesis we study the effect it has on the statistical properties of additive functionals of the Ornstein-Uhlenbeck process and Brownian motion. In this introduction we define resetting, motivate its study and summarize some recent results. Resetting occurs in a variety of contexts. A discussion of these is given in the introduction of Chapter 2. One example is the famous PageRank algorithm [8]. In this algorithm a random walker moves on a graph representing the World Wide Web. An initial probability distribution is placed on the set of nodes and, as the walker makes its way through the graph, the distribution is updated. The walker restarts from a node drawn uniformly at random at a constant rate $r \in (0, \infty)$.

§1.1 Stochastic Resetting

In this section we introduce resetting and collect some basic results following [6]. We consider a homogeneous continuous-time Markov process $\{X_t : t \in [0, \infty)\}$ taking values in a Borel space $(E, \mathcal{E})$, characterized by its initial position x_0 and its transition density $P(t, x, \mathrm{d}y)$, with the following properties:

(a) $P(t, x, \cdot)$ is a probability measure on E.

(b) $P(0, x, \Gamma) = 1\{x \in \Gamma\}$ for any $\Gamma \subset E$.

(c) For each $\Gamma \in \mathcal{E}$ and $t \in [0, \infty)$, $P(t, x, \Gamma)$ is jointly measurable w.r.t. $(t, x) \in [0, \infty) \times E$.

(d) $P(t, x, \mathrm{d}y)$ satisfies the Chapman-Kolmogorov equation

$$P(t + s, x, \Gamma) = \int_E P(s, y, \Gamma) P(t, x, \mathrm{d}y). \tag{1.1.1}$$

Throughout the sequel, all processes live on the same probability space $(\Omega, \mathcal{F}, P)$. Resetting modifies $\{X_t : t \in [0, \infty]\}$ to a new Markov process $\{X^r(t) : t \in [0, \infty)\}$ that restarts from a point in E drawn from a probability distribution $\gamma(\Gamma)$ after an exponentially distributed random time with mean $1/r$, i.e., the number of restarts is represented by a standard Poisson process with rate $r > 0$, independently of $\{X(t) : t \in [0, \infty)\}$. In the following theorem (Theorem 1 of [6]) we express the transition function of the modified process in terms of the transition function of the original process.

1.1.1 Theorem. *The transition function for the modified Markov process* $\{X^r(t), t \in [0, \infty)\}$ *is given by*

$$P^r_\gamma(t, x, \Gamma) = \mathrm{e}^{-rt} P(t, x, \Gamma) + \int_E \gamma(\mathrm{d}y) \int_0^t \mathrm{d}s \, \lambda \mathrm{e}^{-rs} P(s, y, \Gamma). \tag{1.1.2}$$

The proof of this theorem is instructive for understanding the effect of resetting.

Proof. If we define the number of resets up to time t to be $N(t)$ and the times of the resets to be $\{\tau_i\}_{i=1}^{N(t)}$, then we can write the time since the last reset as $t - \tau_{N(t)}$. The transition function of the modified process can be written as the sum of the probability of reaching the set Γ without having been reset and the probability of reaching this set having been reset at least once:

$$\begin{aligned} P_\gamma^r(t,x,\Gamma) =& P\big[\{X_t^r \in \Gamma\} \cap \{N(t)=0\} | X_0^r = 0\big] \\ &+ P\big[\{X_t^r \in \Gamma\} \cap \{N(t)>0\} | X_0^r = 0\big]. \end{aligned} \tag{1.1.3}$$

The first term is the probability of the unmodified process reaching the set Γ multiplied by the probability of not resetting up to time t, i.e.,

$$P\big[\{X_t^r \in \Gamma\} \cap \{N(t)=0\} | X_0^r = 0\big] = \mathrm{e}^{-rt} P(t,x,\Gamma). \tag{1.1.4}$$

For the second term we must integrate the transition function of the unmodified process over all the possible starting positions after the last reset (distributed according to γ) and integrate over all possible lengths of time since the last reset with the appropriate probability density of this time occurring, i.e.,

$$P\big[\{X_t^r \in \Gamma\} \cap \{N(t)>0\} | X_0^r = 0\big] = \int_E \mathrm{d}y \int_0^t \mathrm{d}F(s)\, P(s,y,\Gamma), \tag{1.1.5}$$

where $F(s) = P[t - \tau_{N(t)} \leq s | N(t) > 0]$. Given that $N(t) = n > 0$, the reset times $\{\tau_i\}_{i=1}^n$ are distributed uniformly over the interval $(0,t)$, so that

$$P[\tau_n \leq t - s | N(t) = n] = \Big(\frac{t-s}{t}\Big)^n, \quad n \in \mathbb{N}, \tag{1.1.6}$$

or

$$P[t - \tau_{N(t)} \leq s | N(t) = n] = 1 - \Big(\frac{t-s}{t}\Big)^n, \quad n \in \mathbb{N}. \tag{1.1.7}$$

To calculate $F(s)$ we must sum over n and multiply by the probability of seeing n resets:

$$F(s) = \sum_{n=1}^{\infty} \frac{(rt)^n}{n!} \mathrm{e}^{-rt} \Big[1 - \Big(\frac{t-s}{t}\Big)^n\Big] = 1 - \mathrm{e}^{-rs}. \tag{1.1.8}$$

To complete the proof, we substitute (1.1.8) into (1.1.5) to obtain

$$P\big[\{X_t^r \in \Gamma\} \cap \{N(t)>0\} | X_0^r = 0\big] = \int_E \gamma(\mathrm{d}y) \int_0^t \mathrm{d}s\, \lambda\, \mathrm{e}^{-rs} P(s,y,\Gamma). \tag{1.1.9}$$

□

Considering the case where $E = \mathbb{R}$, we can use (1.1.2) to obtain an expression for the moments, namely,

$$E_{x_0}[(X_t^r)^k] = \mathrm{e}^{-rt} E_{x_0}[X_t^k] + \int_E \gamma(\mathrm{d}y) \int_0^t \mathrm{d}s\, r\, \mathrm{e}^{-rs} E_y[X_s^k], \tag{1.1.10}$$

where E_{x_0} is expectation w.r.t. the process with initial position x_0. Here we assume that the order of integration is interchangeable, which is the case for example when

$$\int_E \gamma(\mathrm{d}y) \int_0^t \mathrm{d}s\, r\, \mathrm{e}^{-rs} E_y[|X_s^k|] < \infty. \tag{1.1.11}$$

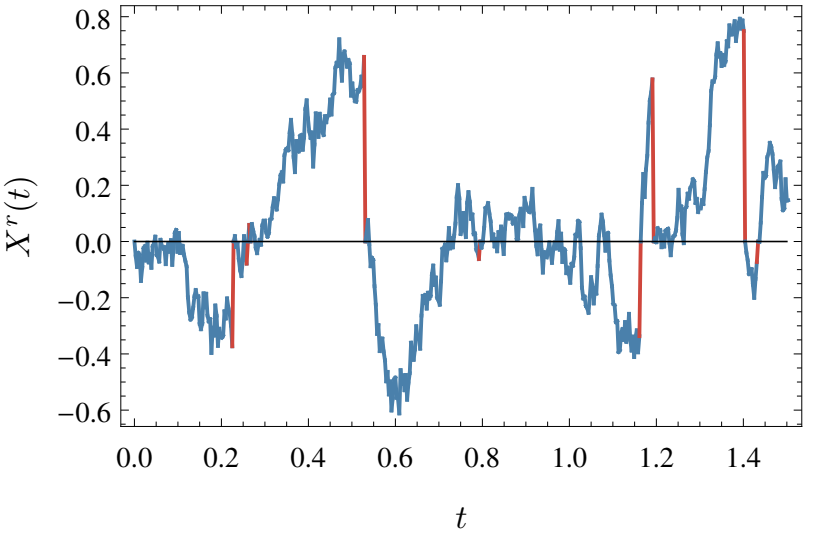

Figure 1.1: Brownian motion with drift $\mu = 0$, noise intensity $\sigma = 1$, resetting rate $r = 5$ and reset position $x_0 = 0$. The reset events are marked by red lines.

§1.2 Example

To illustrate Theorem 1.1.1, we take Brownian motion on $\mathbb{R}$ with drift μ and noise intensity σ on $\mathbb{R}$ (see e.g., [113]). We also take the distribution of the reset point to be a delta-measure concentrated at 0. The stochastic differential equation is

$$\mathrm{d}X_t = \mu \mathrm{d}t + \sigma \mathrm{d}W_t, \quad X_0 = x_0 = 0, \tag{1.2.1}$$

where W_t is standard Brownian motion. Fig. 1.1 shows a simulation of reset Brownian motion.

The probability density function of the process defined by (1.2.1) is

$$p(t, 0, z) = \frac{1}{\sqrt{2\pi\sigma^2 t}} \exp\left(-\frac{(z-\mu t)^2}{2\sigma^2 t}\right), \tag{1.2.2}$$

which does not converge to a proper probability density as $t \to \infty$. By formula (1.1.2), we have

$$\begin{aligned} p^r(t, 0, z) = &\exp(-rt)\frac{1}{\sqrt{2\pi\sigma^2 t}} \exp\left(-\frac{(z-\mu t)^2}{2\sigma^2 t}\right) \\ &+ r\int_0^t \exp(-rs)\frac{1}{\sqrt{2\pi\sigma^2 s}} \exp\left(-\frac{(z-\mu s)^2}{2\sigma^2 s}\right) \mathrm{d}s, \end{aligned} \tag{1.2.3}$$

which has limiting probability density function

$$p^r(z) = r\frac{1}{\sqrt{2r\sigma^2 + \mu^2}} \exp\left[z\left(\mu - \sqrt{2r\sigma^2 + \mu^2}\right)/\sigma^2\right]. \tag{1.2.4}$$

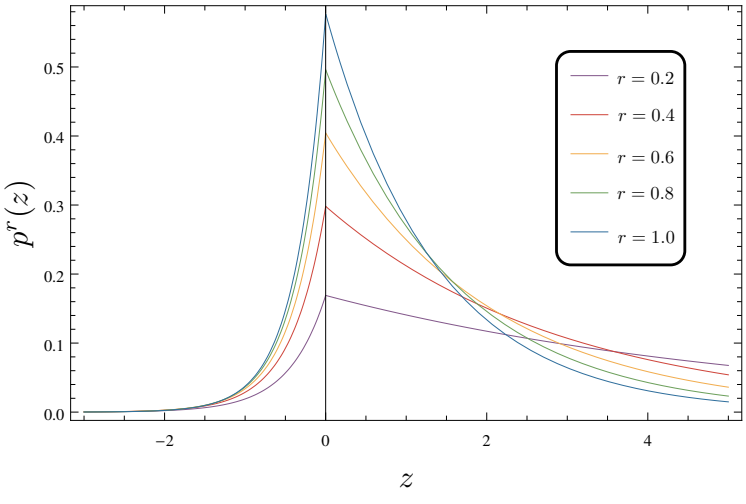

Figure 1.2: $z \mapsto p^r(z)$ for different values of the resetting rate r (with $\mu = 1$, $\sigma = 1$).

Plotting this for different values of r, we see that resetting has a confining effect on the process, as can be seen in Fig. 1.2.

Let us now consider $x \in \mathbb{R}$ and restarting according to the distribution $\gamma(\mathrm{d}y)$. If γ has a finite second moment, then we can calculate the first and second moment of the modified process by using formula (1.1.10) with $E_x[X(t)] = x + \mu t$:

$$\begin{aligned} E_x[X^r(t)] &= \mathrm{e}^{-rt}(x + \mu t) + \int_E \gamma(\mathrm{d}y) \int_0^t \mathrm{d}s\, r\, \mathrm{e}^{-rs}(y + \mu s) \\ &= \mathrm{e}^{-rt}(x + \mu t) + [1 - \mathrm{e}^{-rt}] \int_E \gamma(\mathrm{d}y)\, y + [1 - (1 + rt)\mathrm{e}^{-rt}] \frac{\mu}{r}. \end{aligned} \tag{1.2.5}$$

Here

$$\lim_{t\to\infty} E_x[X_t^r] = \int_E \gamma(\mathrm{d}y)\, y + \frac{\mu}{r}. \tag{1.2.6}$$

A similar calculation gives

$$\lim_{t\to\infty} E_x[(X_t^r)^2] = \frac{\sigma^2}{r} + \frac{2\mu^2}{r^2} + \int_E \gamma(\mathrm{d}y) \left(\frac{2\mu y}{r} + y^2 \right), \tag{1.2.7}$$

so that

$$\lim_{t\to\infty} \mathrm{Var}_x[(X_t^r)^2] = \int_E \gamma(\mathrm{d}y)\, y^2 - \Big(\int_E \gamma(\mathrm{d}y)\, y \Big)^2 + \frac{\sigma^2}{r} + \frac{\mu^2}{r^2}. \tag{1.2.8}$$

Note that the first two terms in the r.h.s. of (1.2.8) equal the variance of the distribution γ for the reset point. These results are similar in nature to the results presented in Chapter 3.

§1.3 Recent Results

The recent work on resetting is difficult to summarize, as the perspectives and contexts in which it is being carried out are so varied. We will focus on two of these perspectives here. The first is the use of resetting in order to improve the efficiency of diffusive searchers and the second is the use of resetting as a mechanism modeling the accidental or deliberate clearing of queues or catastrophes wiping out a population of individuals in a birth-death process.

Search efficiency

In [48] the authors consider the hitting time of a target of a diffusive searcher undergoing resets at rate r. They consider three generalizations of the reset mechanism outlined above. The first is to have a resetting rate dependent on the spatial position of the searcher. The second is to have the reset position be random by drawing it from a distribution every time a reset occurs. The third is to have the target drawn from a distribution. The first result in [48] is the mean first-passage time (at the origin) of a diffusive searcher being reset to position x_r, which is shown to be

$$T(x_r) = \frac{1}{r}\Big[\exp\left(\sqrt{r/\sigma}x_r\right) - 1\Big], \tag{1.3.1}$$

where σ is the noise intensity. For a given x_r, one can calculate the optimal resetting rate in order to minimize the mean first-passage time. Having a space-dependent resetting rate makes it difficult to solve the problem of the mean first-passage time in general. A solvable example is when the resetting rate is set to zero in a window of width a around the reset position x_r and set to a constant outside this window. This leads to an expression for $T(x_r)$ from which one can obtain the optimal resetting rate. In this case it is advantageous to have the window around the reset point only when the target is sufficiently far away from the reset position.

The last generalization is to both have the process reset to a position drawn from a distribution $\mathcal{P}(x_r)$ and to draw the target site x_T from the distribution $P_T(x_T)$. It is convenient to draw the initial position from the same distribution as the reset position. The stationary distribution is

$$p^*(x) = \frac{\alpha_0}{2}\int_{\mathbb{R}} \mathrm{d}z\, \mathcal{P}(z)\exp(-\alpha_0|x-z|), \tag{1.3.2}$$

where $\alpha_0 = \sqrt{r/\sigma}$. The mean first-passage time of a target site x_T is

$$T(x_T) = \frac{1}{r}\Big[\frac{\alpha_0}{2}\frac{1}{p^*(x_T)} - 1\Big], \tag{1.3.3}$$

which, after we average over possible target sites, gives

$$\overline{T} = \frac{1}{r}\Big[\frac{\alpha_0}{2}\int_{\mathbb{R}} \mathrm{d}x_T \frac{P_T(x_T)}{p^*(x_T)} - 1\Big]. \tag{1.3.4}$$

As an example one can take the target to be distributed exponentially

$$P_T(x) = \frac{\beta}{2}\mathrm{e}^{-\beta|x|}, \tag{1.3.5}$$

where $\beta > 0$ is a parameter. If $\beta < 2\alpha_0$, then the optimal resetting distribution is

$$\mathcal{P}(x) = \frac{\beta}{4}\mathrm{e}^{-\beta|z|/2}\Big[1 - \frac{\beta^2}{4\alpha_0^2}\Big] + \frac{\beta^2}{4\alpha_0^2}\delta(z). \tag{1.3.6}$$

If $\beta > 2\alpha_0$, then the authors can prove that taking the reset distribution as $\mathcal{P}(x) = \delta(x)$ is an optimal solution, at least locally.

Birth-death processes with catastrophes

In contrast to the paper discussed before, where the state space is continuous, the birth-death process with catastrophes is an example of a discrete process with resetting. There have been many recent studies on these types of processes [30] [29], [127], [23], [43]. An instructive paper is [30], which studies the first occurrence of an *effective catastrophe*, i.e., a catastrophe while the process is in a state other than the zero state. To make this more concrete, consider the process $\{N(t) : t \in [0, \infty)\}$ that takes values in $\mathcal{S} = \{0, 1, 2, \ldots\}$. Births occur with rate $a_n, n = 0, 1, \ldots$ and deaths with rate $b_n, n = 1, 2, \ldots$. Catastrophes occur with rate ξ, and immediately place the process in the state 0. Define the transition probabilities

$$p_{j,n}(t) = \mathbb{P}[N(t) = n | N(0) = j] \tag{1.3.7}$$

and denote by $\hat{p}_{j,n}(t)$ the same probability, but for $\hat{N}(t)$, which is the same as $N(t)$ with $\xi = 0$, i.e., without catastrophes. Denote the Laplace transform of $p_{j,n}(t)$ and $\hat{p}_{j,n}(t)$ by $\pi_{j,n}(\lambda)$ and $\hat{\pi}_{j,n}(\lambda)$, respectively. The process, $N(t)$, allows catastrophes to occur while in the zero state. Paper [30] considers only effective catastrophes, by which are meant catastrophic transitions from a positive state. A modified process $\{M(t); t \geq 0\}$ on the state space $\{-1, 0, 1, \ldots\}$, is introduced that is identical to $N(t)$, except that catastrophes place the process in the state -1. Denote by $h_{j,n}(t)$ and $\eta_{j,n}(\lambda)$ the analogue of $p_{j,n}(t)$ and $\pi_{j,n}(\lambda)$, respectively. The following theorem [30, Theorem 3.1] gives a relation between the modified process and the birth-death process without catastrophes.

1.3.1 Theorem. *For all $j \in \mathcal{S}$ and $\lambda > 0$,*

$$\eta_{j,-1}(\lambda) = \frac{\xi}{\lambda + \xi}\Big[\frac{1}{\lambda} - \frac{\hat{\pi}_{j,0}(\lambda + \xi)}{1 - \xi\hat{\pi}_{0,0}(\lambda + \xi)}\Big], \tag{1.3.8}$$

$$\eta_{j,n}(\lambda) = \hat{\pi}_{j,n}(\lambda + \xi) + \xi\hat{\pi}_{0,n}(\lambda + \xi)\frac{\hat{\pi}_{j,0}(\lambda + \xi)}{1 - \xi\hat{\pi}_{0,0}(\lambda + \xi)}. \tag{1.3.9}$$

Let $C_{j,0}$ denote the time of the first effective catastrophe given that the process started in state j. The following proposition [30, Proposition 3.2] gives the expected value and variance of $C_{j,0}$.

1.3.2 Proposition. *For all $j \in \mathcal{S}$,*

$$\mathbb{E}[C_{j,0}] = \frac{1}{\xi} + \frac{\hat{\pi}_{j,0}(\xi)}{1 - \xi\hat{\pi}_{0,0}(\xi)}, \tag{1.3.10}$$

$$\begin{aligned}\mathrm{Var}[C_{j,0}] = \frac{1}{\xi^2}\Big\{1 - \frac{\xi^2\hat{\pi}_{j,0}^2(\xi)}{(1-\xi\hat{\pi}_{0,0}(\xi))^2} - \frac{2\xi^2}{1-\xi\hat{\pi}_{0,0}(\xi)}\frac{\mathrm{d}}{\mathrm{d}\xi}\hat{\pi}_{j,0}(\xi) \\ - \frac{2\xi^3\hat{\pi}_{j,0}(\xi)}{(1-\xi\hat{\pi}_{0,0}(\xi))^2}\frac{\mathrm{d}}{\mathrm{d}\xi}\hat{\pi}_{j,0}(\xi)\Big\}.\end{aligned} \tag{1.3.11}$$

Taking the first visit time $T_{j,0} = \inf\{t \geq 0 : N(t) = 0\}$ given that the process started in state j, in contrast we get

$$\mathbb{E}[T_{j,0}] = \frac{1}{\xi}[1 - \hat{\gamma}_{j,0}(\xi)], \tag{1.3.12}$$

$$\mathrm{Var}[T_{j,0}] = \frac{1}{\xi^2}\Big[1 - \hat{\gamma}_{j,0}^2(\xi) + 2\xi\frac{\mathrm{d}}{\mathrm{d}\xi}\hat{\gamma}_{j,0}(\xi)\Big], \tag{1.3.13}$$

where $\hat{\gamma}_{j,0}$ denotes the Laplace transform of the probability density function $\hat{g}_{j,0}(t) = \frac{\mathrm{d}}{\mathrm{d}t}\mathbb{P}[\hat{T}_{j,0} \leq t]$ of the first visit time of the process $\hat{N}(t)$, i.e., without catastrophes. These results are similar in nature to the main result of Chapter 2 and serve to illustrate how delicate discrete versions of processes with resetting are to even slight changes in their definition.

§1.4 Main results of Part I

Modification of a diffusion process by resetting has interesting consequences. Most of the studies so far have investigated the effect on the distribution of the position, or moments thereof. The focus of part I of the thesis is to derive some general results in the spirit of (1.1.2) for additive functionals of the process, namely,

$$F_T = \int_0^T \mathrm{d}t\, f(X_t^r), \tag{1.4.1}$$

with f an $\mathbb{R}$-valued measurable function. From the proof of Theorem 1.1.1 it is clear that the distribution of the position only depends on when the last reset took place. The history of the process before the last reset is irrelevant. This is not the case when we consider the distributions of additive functionals, and this complicates the analysis.

Results of Chapter 2

In Chapter 2, using a renewal argument, we derive a relationship between the Laplace transformed generating functions for additive observables of processes with and without resetting. Let F_T be as above. Then its generating function is

$$G_r(k, T) = \mathbb{E}_r\big[\mathrm{e}^{kF_T}\big], \qquad k \in \mathbb{R},\, T \in [0, \infty), \tag{1.4.2}$$

where $\mathbb{E}_r$ is the expectation with respect to the reset process with reset rate r. The Laplace transform of this function is defined as

$$\tilde{G}_r(k,s) = \int_0^\infty \mathrm{d}T\, \mathrm{e}^{-sT}\, G_r(k,T), \qquad k \in \mathbb{R},\ s \in [0,\infty). \tag{1.4.3}$$

The main result is

1.4.1 Theorem. *If $r\tilde{G}_0(k, s+r) < 1$, then*

$$\tilde{G}_r(k,s) = \frac{\tilde{G}_0(k,s+r)}{1 - r\tilde{G}_0(k,s+r)}. \tag{1.4.4}$$

This allows us to make statements about the large deviation behaviour of the process with resetting based on the behaviour of the process without resetting. We illustrate the usefulness of this theorem by applying it to the average area covered by the Ornstein-Uhlenbeck process defined as

$$A_T = \frac{1}{T}\int_0^T \mathrm{d}t\, X_t \tag{1.4.5}$$

where the Orsntein-Uhlenbeck process is

$$\mathrm{d}X_t = -\gamma X_t \mathrm{d}t + \sigma \mathrm{d}W_t, \tag{1.4.6}$$

γ is the friction coefficient, σ is the noise intensity and W_t is standard Brownian motion. The probability of seeing rare events is characterized by the large deviation rate function $I_r(a)$ through the large deviation principle

$$P(A_T = a) = \mathrm{e}^{-TI_r(a)+o(T)}. \tag{1.4.7}$$

We are able to identify the large deviation rate function with resetting for different reset positions x_r, and compare it to the rate function without resetting as seen in Fig. 1.3.

Chapter 2 is based on [92] and differs in style from the rest of the thesis as it is written for a physics journal.

Results of Chapter 3

In Chapter 3 we identify the large deviation rate function for additive functionals of Brownian motion with reset (rBM), χ_r, in the form of a variational formula in terms of the rate functions of the three constituent processes underlying F_T (where we replace X_t^r by the standard Brownian motion with reset W_t^r), namely (see [40, Chapters I-II]):

(1) The rate function for $(T^{-1}N(T))_{T>0}$, the number of resets per unit of time:

$$I_r(n) = n\log\left(\frac{n}{r}\right) - n + r, \qquad n \in [0,\infty). \tag{1.4.8}$$

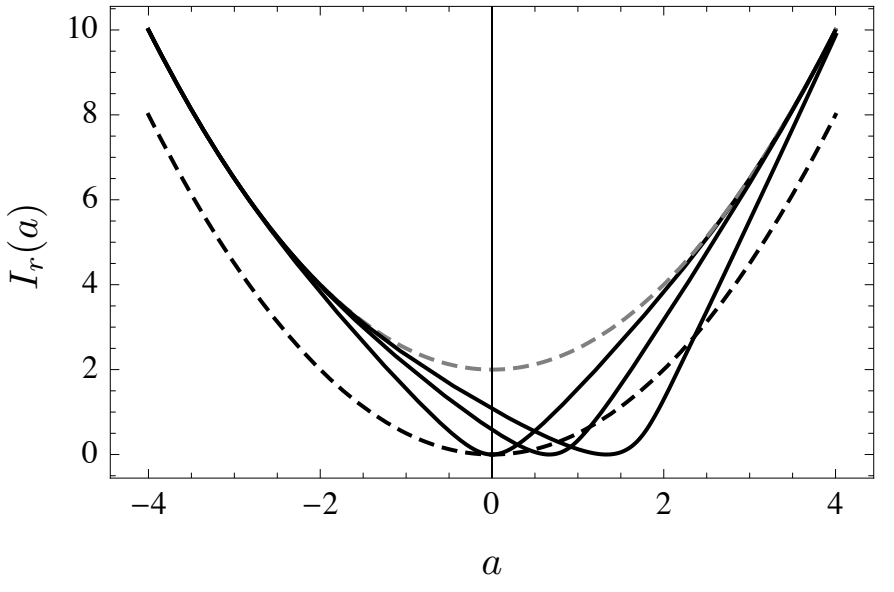

Figure 1.3: Black curves: $I_r(a)$ for $x_r = 0, 1, 2$ (from left to right). Dashed black curve: Non-reset rate function $I_0(a)$. Dashed gray curve: Tail approximation of $I_r(a)$. Parameters: $r = 2$, $\gamma = 1$, $\sigma = 1$.

(2) The rate function for $(N^{-1}\sum_{i=1}^{N}\delta_{\tau_i})_{N\in\mathbb{N}}$, the empirical distribution of the duration of the reset periods:

$$J_r(\mu) = h(\mu \mid \mathcal{E}_r), \qquad \mu \in \mathcal{P}([0,\infty)). \tag{1.4.9}$$

Here, $\mathcal{P}([0,\infty))$ is the set of probability distributions on $[0,\infty)$, $\mathcal{E}_r$ is the exponential distribution with mean $1/r$, and $h(\cdot \mid \cdot)$ denotes the relative entropy

$$h(\mu \mid \nu) = \int_0^\infty \mu(dx) \log\left[\frac{\mathrm{d}\mu}{\mathrm{d}\nu}(x)\right], \qquad \mu,\nu \in \mathcal{P}([0,\infty)). \tag{1.4.10}$$

(3) The rate function for $(N^{-1}\sum_{i=1}^{N}F_{\tau,i})_{N\in\mathbb{N}}$, the empirical average of i.i.d. copies of the *reset-free* functional F_τ over a time τ:

$$K_\tau(u) = \sup_{v\in\mathbb{R}}\{uv - M_\tau(v)\}, \qquad u \in \mathbb{R},\ \tau \in [0,\infty). \tag{1.4.11}$$

Here, $M_\tau(v) = \log \mathbb{E}_0\big[\mathrm{e}^{vF_\tau}\big]$ is the cumulant generating function of F_τ without reset and we require, for all $\tau \in [0,\infty)$, that M_τ exists in an open neighbourhood of 0 in $\mathbb{R}$. It is known that K_τ is smooth and strictly convex on the interior of its domain (see [40, Chapter I]).

1.4.2 Theorem. *For every $r > 0$, the family $(\mathbb{P}_r(T^{-1}F_T \in \cdot\,))_{T>0}$ satisfies the LDP on $\mathbb{R}$ with speed T and with rate function χ_r given by*

$$\chi_r(\phi) = \inf_{(n,\mu,w)\in\Phi(\phi)}\Big\{I_r(n) + nJ_r(\mu) + n\int_0^\infty \mu(\mathrm{d}t)\, K_t(w(t))\Big\}, \qquad \phi \in \mathbb{R}, \tag{1.4.12}$$

where

$$\Phi(\phi) = \left\{ (n,\mu,w) \in [0,\infty) \times \mathcal{P}([0,\infty)) \times \mathcal{B}([0,\infty);\mathbb{R}) \colon\ n \int_0^\infty \mu(\mathrm{d}t)\, w(t) = \phi \right\} \tag{1.4.13}$$

with $\mathcal{B}([0,\infty);\mathbb{R})$ *the set of Borel-measurable functions from* $[0,\infty)$ *to* $\mathbb{R}$.

A general result deduced from the variational formula shows that the rate function for functionals of rBM (under the additional assumption that the mean without resetting diverges) is zero above the mean and quadratic below but close to the mean. Define

$$\phi_r^* = \lim_{T\to\infty} \mathbb{E}_r[T^{-1}F_T], \qquad r \geq 0. \tag{1.4.14}$$

1.4.3 Theorem. *Suppose that* f *is such that*

$$\mathbb{E}[f(W_t)^2] \leq C\mathbb{E}[f(W_t)]^2 \quad \forall t \geq 0 \tag{1.4.15}$$

and that $\phi_0^* = \infty$. *For every* $r > 0$, *if* $\phi_r^* < \infty$, *then*

$$\chi_r(\phi) = 0 \quad \forall\, \phi \geq \phi_r^*. \tag{1.4.16}$$

1.4.4 Theorem. *Suppose that* $\phi_0^* = \infty$. *For every* $r > 0$, *if* $\phi_r^* < \infty$, *then*

$$\chi_r(\phi) \sim C_r(\phi_r^* - \phi)^2, \qquad \phi \uparrow \phi_r^*, \tag{1.4.17}$$

with $C_r \in (0,\infty)$ *a constant that is given by a variational formula. (The symbol* $\sim$ *means that the quotient of the left-hand side and the right-hand side tends to* 1.*)*

For the positive occupation time of rBM defined by

$$A_T = \int_0^T 1_{[0,\infty)}(W_t^r)\,\mathrm{d}t \tag{1.4.18}$$

we find an explicit expression of the density.

1.4.5 Theorem. *The positive occupation time of rBM has density*

$$p_r^A(a) = \frac{r}{T}\,\mathrm{e}^{-rT}\, W\big(r\sqrt{a(T-a)}\,\big), \qquad a \in (0,T), \tag{1.4.19}$$

where

$$W(x) = \frac{1}{x}\sum_{j=0}^{\infty} \frac{x^j}{\Gamma(\frac{j+1}{2})^2} = I_0(2x) + \frac{1}{x\pi}\,{}_1F_2\big(\{1\},\{\tfrac{1}{2},\tfrac{1}{2}\},x^2\big), \qquad x \in (0,\infty), \tag{1.4.20}$$

with $I_0(y)$ *the modified Bessel function of the first kind with index* 0 *and* ${}_1F_2(\{a\},\{b,c\},y)$ *the generalized hypergeometric function* [2, Section 9.6, Formula 15.6.4].

For the area covered by rBM defined by

$$B_T = \int_0^T W_t^r\,\mathrm{d}t \tag{1.4.21}$$

we prove the following central limit theorem.

1.4.6 Theorem. *The area of rBM satisfies the central limit theorem,*

$$\lim_{T\to\infty} \sigma\sqrt{T}\; p_r^B\left(\frac{b}{\sigma\sqrt{T}}\right) = N(0,1) \tag{1.4.22}$$

with $N(0,1)$ the standard Gaussian distribution and $\sigma = 2/r^2$.

Here we denote by $p_r^B(b)$, $b \in \mathbb{R}$, the density of the area of rBM with respect to the Lebesgue measure.

For the absolute area of rBM, defined as

$$C_T = \int_0^T |W_t^r|\,\mathrm{d}t, \tag{1.4.23}$$

whose density with respect to the Lebesgue measure is denoted by $p_r^C(c)$, $c \in [0,\infty)$, we calculate the mean and variance.

1.4.7 Theorem. *The absolute area of rBM has a mean and a variance given by*

$$\mathbb{E}_r[C_T] = T^{3/2} f_1(rT), \qquad \mathrm{Var}_r[C_T] = T^3 f_2(rT), \qquad r > 0, \tag{1.4.24}$$

where

$$f_1(\rho) = \frac{1}{\sqrt{2\pi}}\left[\frac{\mathrm{e}^{-\rho}}{\rho} + \frac{\sqrt{\pi}}{2(\rho)^{3/2}}\,(2\rho-1)\,\mathrm{erf}[\sqrt{\rho}\,]\right] \tag{1.4.25}$$

and

$$f_2(\rho) = \frac{1}{8\pi(\rho)^3}\left[2\pi\left(2\rho^2+\rho-6+(5\rho+6)\mathrm{e}^{-\rho}\right) - \left(2\sqrt{\rho}\,\mathrm{e}^{-\rho} + \sqrt{\pi}(2\rho-1)\,\mathrm{erf}[\sqrt{\rho}]\right)^2\right]. \tag{1.4.26}$$

Furthermore we give an explicit representation of the rate function of $(T^{-1}C_T)_{T>0}$ for values below its mean.

1.4.8 Theorem. *Let $c_r^* = 1/\sqrt{2r}$, and let s_k^* be the largest real root in s of the equation*

$$\frac{r}{(-k)^{2/3}} H\left(\frac{2^{1/3}(s+r)}{(-k)^{2/3}}\right) = 1, \qquad k < 0. \tag{1.4.27}$$

Then $(T^{-1}C_T)_{T>0}$ satisfies the LDP on $(0, c_r^*)$ with speed T and with rate function given by the Legendre transform of s_k^*.

Here the function $H(\cdot)$ is defined by

$$H(x) = -2^{1/3}\frac{\mathrm{AI}(x)}{\mathrm{Ai}'(x)}, \tag{1.4.28}$$

where

$$\mathrm{AI}(x) = \int_x^\infty \mathrm{Ai}(t)\,\mathrm{d}t \tag{1.4.29}$$

is the integral Airy function and $\mathrm{Ai}(x)$ is the Airy function [2, Section 10.4] defined, for example, by

$$\mathrm{Ai}(x) = \frac{1}{\pi} \int_0^\infty \cos\left(\tfrac{1}{3}t^3 + xt\right)\, \mathrm{d}t. \tag{1.4.30}$$

Chapter 3 is based on [52].

Open Problems

The most interesting challenge is to extend the above theorems to additive functionals of random walks on random graphs with reset. This is particularly interesting in the context of the PageRank algorithm, which computes the stationary distribution of webpages through a random walk with reset along these webpages. The large deviation rate function for the local time of this random walk gives information on the rate of convergence of the random walk.

An open problem stated in Chapter 3 is to prove that the rate function for the area of Brownian motion is identically zero. This problem seems deceptively simple, but actually is not.

Part II

The Kuramoto model is a classical model that is used to describe the phenomenon of synchronization of phase oscillators. It has been studied extensively from different perspectives, including mathematics, theoretical physics, computer science and neuroscience. Recently, much heuristic and numerical work has been done on the Kuramoto model on complex networks [110]. Due to the non-linearity of the interaction, analytic results have been scarce. Part of the work has focused on identifying the effect of communities in the underlying network structure of the interactions between the phase oscillators, which determines their ability to synchronize. In Part II of the thesis we study the effect of community structure analytically in two simple cases, namely, a hierarchical network and a two-community network. In this introduction we define the Kuramoto model, outline some of the recent results in the mathematical literature, and summarize what has been done in the context of complex networks.

§1.5 The Stochastic Kuramoto model

The Kuramoto model was introduced by Yoshiki Kuramoto in 1975 to model the phenomenon of synchronization. Synchronization had fascinated scientists since Christiaan Huygens observed 'an odd kind of sympathy' between the pendulums of his clocks designed for time-keeping on ships in the 17^{th} century. The novelty of the Kuramoto model was that it captured the essence of synchronization while being simple enough to be exactly solvable. Examples of synchronization in nature are copious and consequently the number of models proposed to describe them is overwhelming. To mention but a few, synchronization is often observed among populations of insects, for example crickets chirping and fireflies flashing. It also controls circadian rhythms, power-grids and, to end with the most relevant example for this thesis, the suprachiasmatic nucleus (the body-clock), which is a cluster of neurons in the brain of mammals.

The stochastic version of the model describes the evolution of oscillators on a one-dimensional sphere $\mathbb{S}$ that interact in a mean-field way. Each oscillator θ_i has its own intrinsic frequency ω_i, which is drawn from a common distribution $\mu(\omega)$ on $\mathbb{R}$. The interaction between two oscillators is given by the sine of their phase difference. Mathematically this is given by a system of coupled stochastic differential equations:

$$\mathrm{d}\theta_i(t) = \omega_i \mathrm{d}t + \frac{K}{N}\sum_{j=1}^{N} \sin(\theta_j(t) - \theta_i(t))\mathrm{d}t + D\mathrm{d}W_i(t), \quad i = 1, \ldots, N. \tag{1.5.1}$$

Here, K is the interaction strength, $D > 0$ is the noise strength, and $(W_i(t))_{t\geq 0, i=1,\ldots,N}$ are independent standard Brownian motions. The oscillators are initially identically distributed according to some law on $\mathbb{S}$.

The elegance of this model comes from the choice of the order parameter:

1.5.1 Definition (Order parameter).

$$r_N(t)\mathrm{e}^{i\psi_N(t)} = \frac{1}{N}\sum_{j=1}^{N}\mathrm{e}^{i\theta_j(t)}. \tag{1.5.2}$$

This enables one to write the evolution equations as

$$\mathrm{d}\theta_i(t) = \omega_i\mathrm{d}t + Kr_N(t)\sin(\psi_N(t)-\theta_i(t))\mathrm{d}t + D\mathrm{d}W_i(t), \quad i=1,\dots,N. \tag{1.5.3}$$

The order parameter can be understood as measuring the amount of synchronization, given by $r(t)\in[0,1]$, and the average phase angle, given by $\psi(t)\in[0,2\pi)$. Equation (1.5.3) shows that the amount of synchronization modulates the strength at which oscillators interact with the average phase angle.

In the thesis we deal mainly with the non-disorderd case, which corresponds to the choice $\mu(\omega)=\delta_0$ i.e., all oscillators have natural frequency 0. In this case the model is reversible, which is a major simplification. The Gibbs measure under which it is reversible is given by

$$\frac{1}{Z_{N,K}}\exp\Big(-2KH_N(\theta_1,\dots,\theta_N)\Big)\mathrm{d}\theta_1\dots\mathrm{d}\theta_N, \tag{1.5.4}$$

where the Hamiltonian is

$$H_N(\theta_1,\dots,\theta_N) = -\frac{1}{2N}\sum_{j=1}^{N}\sum_{i=1}^{N}\cos(\theta_j-\theta_i). \tag{1.5.5}$$

1.5.2 Definition (Empirical measure).

$$\nu_{N,t}(\mathrm{d}\theta) = \frac{1}{N}\sum_{i=1}^{N}\delta_{\theta_i(t)}(\mathrm{d}\theta). \tag{1.5.6}$$

This empirical measure converges weakly to a deterministic process that is absolutely continuous w.r.t. the Lebesgue measure with a density $p(\theta)$ that solves the McKean-Vlasov equation

$$\frac{\partial p(t;\theta)}{\partial t} = \frac{D}{2}\frac{\partial^2 p(t;\theta)}{\partial\theta^2} - \frac{\partial}{\partial\theta}\Big[Kr(t)\sin(\psi(t)-\theta)p(t;\theta)\Big], \tag{1.5.7}$$

where $r(t)$ and $\psi(t)$ are the limits of the order parameter defined in (1.5.2), which satisfy the self-consistency relation

$$r(t)\mathrm{e}^{i\psi(t)} = \int_{\mathbb{S}}\mathrm{d}\theta\,\mathrm{e}^{i\theta}p(t;\theta). \tag{1.5.8}$$

The stationary solutions of the McKean-Vlasov equation exhibit a phase transition in the synchronization level. There is a threshold value for the interaction strength K_c, below which only the stationary solution with zero synchronization is possible and above which synchronization takes on non-zero values as well. This is formalized in the following proposition taken from [80, Section 4.2].

1.5.3 Proposition. *The non-disordered Kuramoto model exhibits a phase transition in the interaction strength parameter K:*

(a) *$K \leq K_c$: There is a unique stationary solution to (1.5.7), called the incoherent solution*

$$p(\theta) = \frac{1}{2\pi}, \quad \theta \in \mathbb{S}. \tag{1.5.9}$$

(b) *$K > K_c$: A circle of synchronized solutions appears in addition to the incoherent solution, namely,*

$$\{p(\cdot + \theta_0) : \theta_0 \in \mathbb{S}\} \tag{1.5.10}$$

with

$$p(\theta) = \frac{1}{Z} \mathrm{e}^{2Kr\cos\theta}, \quad \theta \in \mathbb{S}, \tag{1.5.11}$$

where $Z = \int_{\mathbb{S}} \mathrm{d}\theta\, \mathrm{e}^{2Kr\cos\theta}$.

§1.6 Recent Results

Complex Networks

Studies of the stochastic Kuramoto model on complex networks have appeared only recently. Most are not mathematically rigorous. There have, however, been more general (rigorous) works on interacting diffusions on complex networks [16, 28, 38, 82, 100]. In order to study the Kuramoto model on a complex network, the interaction strength parameter K is replaced by $KA_{i,j}$ with $A_{i,j}, i, j = 1, \ldots, N$, the adjacency matrix of the network. To circumvent technical difficulties it is convenient to consider an annealed version of the model as in [121]. The idea is to approximate the complex network by a complete graph with edge weights given by $\tilde{A}_{i,j}$, in such a way that the weights in the complete graph conserve the degrees of the nodes in the original network, i.e.,

$$k_i = \sum_{j=1}^{N} \tilde{A}_{ij}, \tag{1.6.1}$$

where k_i is the degree of node (oscillator) i in the original network. Typically, k_i are independently and identically distributed according to a probability distribution γ, and the network is taken to be undirected. If the degrees of the network are uncorrelated, then this is simply achieved by setting the edge weights equal to the probability of a node with degree k_i being connected to a node with degree k_j, i.e.,

$$\tilde{A}_{ij} = k_i \frac{k_j}{\sum_{l=1}^{N} k_l}. \tag{1.6.2}$$

Using this approximation in the stochastic Kuramoto model, we get

$$\mathrm{d}\theta_i(t) = \omega_i \mathrm{d}t + \frac{K}{N} \frac{k_i}{\sum_{l=1}^{N} k_l} \sum_{j=1}^{N} k_j \sin(\theta_j(t) - \theta_i(t))\mathrm{d}t + D\mathrm{d}W_i(t), \quad i = 1, \ldots, N, \tag{1.6.3}$$

for which we can define the alternative order parameter

$$r_N(t)\mathrm{e}^{i\psi_N(t)} = \frac{\sum_{j=1}^{N} k_j \mathrm{e}^{i\theta_j(t)}}{\sum_{l=1}^{N} k_l}. \tag{1.6.4}$$

Again this simplifies the model:

$$\mathrm{d}\theta_i(t) = \omega_i \mathrm{d}t + K r_N(t) \frac{k_i}{N} \sin(\psi_N(t) - \theta_i(t))\mathrm{d}t + D\mathrm{d}W_i(t), \quad i = 1, \ldots, N. \tag{1.6.5}$$

Note that how strongly each node is coupled to the mean-field is determined by its degree. Under the additional assumption that phase correlations can be disregarded, the large N limit can be analyzed. In this limit, the density $p(t;\theta|\omega,k)$ of oscillators for a fixed natural frequency ω and a fixed degree k follows a Fokker-Planck equation:

$$\frac{\partial p(t;\theta|\omega,k)}{\partial t} = \frac{D}{2}\frac{\partial^2 p(t;\theta|\omega,k)}{\partial \theta^2} - \frac{\partial}{\partial \theta}\Big[\{\omega + \tilde{K} r(t) k \sin(\psi(t) - \theta)\} p(t;\theta|\omega,k)\Big]. \tag{1.6.6}$$

Here, $\tilde{K} = K/N$ and we have the self-consistency equation

$$r(t)\mathrm{e}^{i\psi(t)} = \frac{1}{\langle k \rangle} \int_{\mathbb{S}} \mathrm{d}\theta \int_{\mathbb{R}} \mu(\mathrm{d}\omega) \int_{k_{\min}}^{\infty} \gamma(\mathrm{d}k)\, \mathrm{e}^{i\theta}\, k\, p(t;\theta|\omega,k) \tag{1.6.7}$$

with $k_{\min}$ the minimum degree in the network and $\langle k \rangle = \int_0^\infty k\gamma(\mathrm{d}k)$ the average degree.

When the natural frequency distribution $\mu(\omega)$ is symmetric and has mean zero, then the critical coupling strength is

$$K_c = 2N\langle k \rangle \Big[\int_{\mathbb{R}} \mu(\mathrm{d}\omega) \int_{k_{\min}}^{\infty} \gamma(\mathrm{d}k) \frac{Dk^2}{D^2 + \omega^2} \Big]^{-1}, \tag{1.6.8}$$

which is divergent with N.

Two-community model

The same authors considered the stochastic Kuramoto model without disorder on a two-community network [120], assigning an in-degree and an out-degree to each node i (oscillator), K_i and G_i, respectively. Grouping these into two populations, one with interaction parameters (K_1, G_1) and one with interaction parameters (K_2, G_2), we get a two-community version. In this case we can define an order parameter and a density for each community. The limiting densities evolve according to

$$\frac{\partial p_{1,2}(t;)\theta}{\partial t} = D\frac{\partial^2 p_{1,2}(t;\theta)}{\partial \theta^2} - \frac{\partial}{\partial \theta}\Big[K_{1,2} R(t) \sin(\Psi(t) - \theta) p_{1,2}(t;\theta)\Big], \tag{1.6.9}$$

where $R(t)$ and $\Psi(t)$ are defined by

$$R(t)\mathrm{e}^{i\Psi(t)} = \frac{1}{2}\big[r_1(t) G_1 \mathrm{e}^{\psi_1(t)} + r_2(t) G_2 \mathrm{e}^{i\psi_2(t)}\big]. \tag{1.6.10}$$

The community synchronization levels $r_{1,2}(t)$ and average phases $\psi_{1,2}(t)$ are defined analogously as before. The phase difference between the average phases is defined by $\delta(t) = \psi_1(t) - \psi_2(t)$. Approximating the populations of the oscillators to be distributed according to a Gaussian distribution ('Gaussian Approximation') amounts to expanding the densities $p_{1,2}(t;\theta)$ in a Fourier series, and replacing real and imaginary components by their Gaussian counterparts, where the mean and variance of the Gaussian are assumed to be time-dependent. Under such an approximation the dynamics of the system can be described by a set of three equations:

$$\dot{r}_1 = -r_1 D + \frac{1-r_1^4}{4} K_1 [r_1 G_1 + r_2 G_2 \cos\delta], \tag{1.6.11}$$

$$\dot{r}_2 = -r_2 D + \frac{1-r_2^4}{4} K_2 [r_2 G_2 + r_1 G_1 \cos\delta], \tag{1.6.12}$$

$$\dot{\delta} = -\frac{\sin\delta}{4} \big[(r_1^{-1} + r_1^3) K_1 r_2 G_2 + (r_2^{-1} + r_2^3) K_2 r_1 G_1 \big]. \tag{1.6.13}$$

To find the possible stationary states, this set of equations, must be solved with the restriction that $\dot{r}_{1,2} = \dot{\delta} = 0$. This leads to the phase diagram given in Fig. 2 of [120], which shows the existence of traveling waves and of states where there is a constant phase lag between the two populations. Further numerical analysis shows that the model is significantly richer when considered on a two-community network.

Superficial hierarchical Kuramoto model

The previous two examples rely on approximations that may well be justified by simulations, but cannot be considered rigorous. Reference [32] considers N copies of the stochastic Kuramoto model and introduces a mean-field interaction between their average phases after they have sufficiently synchronized. This is used as Kuramoto model on the second level. Taking N copies of the second level Kuramoto model with a mean-field interaction of the Kuramoto type gives the third level Kuramoto model. This is repeated. We refer to this as the superficial hierarchical Kuramoto model in order to distinguish it from what we will consider later. The name refers to the fact that the interaction is imposed at the level of the average phases, which is more on the surface than what we will consider. We define the coupling strength at the n^{th} level to be $K^{(n)}$ and the synchronization at the n^{th} level to be $r^{(n)}(t)$. The result relevant to our work is one giving a necessary and sufficient condition for $r^{(n)}$ to be positive in the limit as $n \to \infty$ and $t \to \infty$ ([32] Theorem 1.4.3).

1.6.1 Theorem.

$$\lim_{n\to\infty} r^{(n)} > 0 \iff \sum_{m\in\mathbb{N}} \frac{1}{\gamma^{(m)}} < \infty, \tag{1.6.14}$$

where

$$\gamma^{(n)} = \frac{K^{(n)} (r^{(n-1)})^2}{D^2}, \quad n \in \mathbb{N}. \tag{1.6.15}$$

This seems a strong result, but since the $\gamma^{(n)}$ depend sequentially on the previous levels of synchronization, it is not easy to calculate the sum of their inverses.

§1.7 Discrepancy

The nonlinearity of the interaction in the Kuramoto model greatly increases the difficulty in analyzing the model. This can be illustrated by a discrepancy that arises when considering the Kuramoto model at times of order Nt, i.e., time is scaled by the number of oscillators. Both [32] and [14] prove that the average phase $\psi(t)$ performs a diffusion on this time scale. It is, however, remarkable that the calculation of the quadratic variation of the resulting diffusion via standard Itô-calculus gives an incorrect prediction. Itô's rule applied to (1.5.2) yields the expression

$$\mathrm{d}\psi_{N,t} = \sum_{i=1}^{N} \frac{\partial \psi_{N,t}}{\partial \theta_i}\, \mathrm{d}\theta_i(t) + \frac{1}{2} \sum_{i=1}^{N} \frac{\partial^2 \psi_{N,t}}{\partial \theta_i^2} \left(\mathrm{d}\theta_i(t)\right)^2 \tag{1.7.1}$$

with

$$\begin{aligned} \frac{\partial \psi_{N,t}}{\partial \theta_i} &= \frac{1}{N r_{N,t}} \cos\left[\psi_{N,t} - \theta_i(t)\right], \\ \frac{\partial^2 \psi_{N,t}}{\partial \theta_i^2} &= -\frac{2}{\left(N r_{N,t}\right)^2} \sin\left[\psi_{N,t} - \theta_i(t)\right] \cos\left[\psi_{N,t}(t) - \theta_i(t)\right] \\ &\quad + \frac{1}{N r_{N,t}} \sin\left[\psi_{N,t} - \theta_i(t)\right]. \end{aligned} \tag{1.7.2}$$

Inserting (1.5.3) into (1.7.1)–(1.7.3), we get

$$\mathrm{d}\psi_{N,t} = I(N;t)\, \mathrm{d}t + \mathrm{d}J(N;t) \tag{1.7.3}$$

with

$$\begin{aligned} I(N;t) &= \left[\frac{K}{N} - \frac{1}{\left(N r_{N,t}\right)^2}\right] \sum_{i=1}^{N} \sin\left[\psi_{N,t} - \theta_i(t)\right] \cos\left[\psi_{N,t} - \theta_i(t)\right], \\ \mathrm{d}J(N;t) &= \frac{1}{N r_{N,t}} \sum_{i=1}^{N} \cos\left[\psi_{N,t} - \theta_i(t)\right] \mathrm{d}W_i(t), \end{aligned} \tag{1.7.4}$$

where we use that $\sum_{i=1}^{N} \sin[\psi_{N,t} - \theta_i(t)] = 0$ by (1.5.2). Since the last term is a sum of independent Brownian motions, the asymptotic variance should be given by t/N times

$$\frac{1}{r^2} \int_0^{2\pi} \mathrm{d}\theta\, p(\theta) \cos^2\theta, \tag{1.7.5}$$

where

$$p(\theta) = \frac{\mathrm{e}^{2Kr\cos\theta}}{\int_{\mathbb{S}} \mathrm{d}\theta'\, \mathrm{e}^{2Kr\cos\theta'}} \tag{1.7.6}$$

is the stationary density of the Kuramoto model so that

$$\lim_{t\to\infty} \lim_{N\to\infty} \nu_{N,t}(\mathrm{d}\theta) = p(\theta)\mathrm{d}\theta. \tag{1.7.7}$$

Another way of calculating this variance is to compute the quadratic variation of the random variable that arises when projecting the fluctuations of the measure onto the tangent space of the steady-state manifold. This random variable is defined as

$$Y_t := \frac{\langle\langle \nu_{N,t} - \nu_{N,0}, p' \rangle\rangle}{\langle\langle p', p' \rangle\rangle}, \tag{1.7.8}$$

where $\langle\langle \cdot, \cdot \rangle\rangle$ is the scalar product in the Hilbert space $H_{-1,1/p}$, so that

$$\langle\langle u, v \rangle\rangle = \int_{\mathbb{S}} \mathrm{d}\theta \, \frac{\mathcal{U}(\theta)\mathcal{V}(\theta)}{p(\theta)} \tag{1.7.9}$$

and $\mathcal{U}$ is such that $u = \mathcal{U}'$ with the convention that $\int_{\mathbb{S}} \frac{\mathcal{U}(\theta)}{p(\theta)} \mathrm{d}\theta = 0$. To calculate $\langle\langle p', p' \rangle\rangle$, we define $\mathcal{P}$ so that $\mathcal{P}' = p'$. This means that $\mathcal{P}(\theta) = p(\theta) + C$, where the constant C has to be determined by the convention, which gives

$$C = -\frac{2\pi}{\int_{\mathbb{S}} \mathrm{d}\theta \frac{1}{p(\theta)}}. \tag{1.7.10}$$

Using this formula, we have

$$\langle\langle p', p' \rangle\rangle = \int_{\mathbb{S}} \mathrm{d}\theta \, \frac{\mathcal{P}^2(\theta)}{p(\theta)} = 1 - \frac{(2\pi)^2}{\int_{\mathbb{S}} \mathrm{d}\theta \, \frac{1}{p(\theta)}}. \tag{1.7.11}$$

To calculate the quadratic variation we follow [14] from equation (2.8) to (2.9). We apply Itô's formula to

$$\langle\langle \nu_{N,t} - \nu_{N,0}, p' \rangle\rangle = \int_{\mathbb{S}} \mathrm{d}\theta \, \frac{1}{p(\theta)} \mathcal{P}(\theta)\mathcal{V}_N(\theta), \tag{1.7.12}$$

where $\mathcal{P}$ and $\mathcal{V}_N$ are the appropriate primitives. We can write this as

$$\langle\langle \nu_{N,t} - \nu_{N,0}, p' \rangle\rangle = \int_{\mathbb{S}} \mathrm{d}\theta \, \mathcal{V}_N(\mathrm{d}\theta) \partial_\theta \mathcal{K}(\theta), \tag{1.7.13}$$

where $\mathcal{K}$ is the primitive of $1 - c/p(\theta)$, so that

$$\langle\langle \nu_{N,t} - \nu_{N,0}, p' \rangle\rangle = -\int_{\mathbb{S}} \mathrm{d}\theta \, \mathcal{K}(\theta)[\nu_{N,t}(\mathrm{d}\theta) - p(\theta)]. \tag{1.7.14}$$

Applying Itô's formula, we get

$$\int_{\mathbb{S}} \mathcal{K}(\theta)\nu_{N,t}(\mathrm{d}\theta) - \int_{\mathbb{S}} \mathrm{d}\theta \, \mathcal{K}(\theta)p(\theta) = -K \int_0^t \mathrm{d}s \int_{\mathbb{S}^2} \nu_{N,s}(\mathrm{d}\theta')\nu_{N,s}(\mathrm{d}\theta')\mathcal{K}'(\theta') \sin(\theta - \theta') \tag{1.7.15}$$

$$- \int_0^t \mathrm{d}s \int_{\mathbb{S}} \nu_{N,s}(\mathrm{d}\theta)\mathcal{K}''(\theta) + \sum_{j=1}^{N} \frac{1}{N} \int_0^t \mathcal{K}'(\theta_j(s))\mathrm{d}W_j(s),$$

which is a sum of a drift term and a martingale. We can compute the quadratic variation of the martingale as

$$M_{N,\mathcal{K}}(t) = \sum_{j=1}^{N} \frac{1}{N} \int_0^t \mathcal{K}'(\theta_j(s)) \mathrm{d}W_j(s), \tag{1.7.16}$$

so

$$\langle M_{N,\mathcal{K}} \rangle_t = \sum_{j=1}^{N} \int_0^t \mathrm{d}s \frac{1}{N^2} (\mathcal{K}'(\theta_j(s)))^2 = \frac{1}{N} \int_0^t \mathrm{d}s \int_{\mathbb{S}} \nu_{N,s}(\mathrm{d}\theta)(\mathcal{K}'(\theta))^2. \tag{1.7.17}$$

The integral over $\mathbb{S}$ converges:

$$\lim_{N\to\infty} \int_{\mathbb{S}} \nu_{N,s}(\mathrm{d}\theta)(\mathcal{K}'(\theta))^2 = \int_{\mathbb{S}} \mathrm{d}\theta \, (\mathcal{K}'(\theta))^2 p(\theta), \tag{1.7.18}$$

and since we are starting in the stationary distribution this gives

$$\langle M_{N,\mathcal{K}} \rangle_t = \frac{t}{N} \int_{\mathbb{S}} \mathrm{d}\theta \, (\mathcal{K}'(\theta))^2 p(\theta), \tag{1.7.19}$$

as also stated in [14]. Since $\mathcal{K}$ is the primitive, this says that

$$\int_{\mathbb{S}} \mathrm{d}\theta \Big(1 - \frac{c}{p(\theta)}\Big)^2 = \int_{\mathbb{S}} \mathrm{d}\theta \, p(\theta) - 2c \int_{\mathbb{S}} \mathrm{d}\theta + c^2 \int_{\mathbb{S}} \frac{\mathrm{d}\theta}{p(\theta)} \tag{1.7.20}$$

$$= 1 - 2\frac{(2\pi)^2}{\int_{\mathbb{S}} \mathrm{d}\theta/p(\theta)} + \frac{(2\pi)^2}{\int_{\mathbb{S}} \mathrm{d}\theta/p(\theta)}. \tag{1.7.21}$$

The quadratic variation of Y_t is therefore t/N times

$$\frac{1 - (2\pi)^2 \big[\int_{\mathbb{S}} \frac{\mathrm{d}\theta}{p(\theta)}\big]^{-1}}{\langle\langle p', p' \rangle\rangle^2} = \frac{1}{\langle\langle p', p' \rangle\rangle} = \frac{1}{1 - \frac{(2\pi)^2}{\int \mathrm{d}\theta/p(\theta)}} = \frac{1}{1 - I_0(2Kr)^{-2}}, \tag{1.7.22}$$

where $I_0(\cdot)$ is the modified Bessel function of the first kind

$$I_n(x) = \frac{1}{2\pi} \int_0^{2\pi} \mathrm{d}\theta \, \cos(n\theta) \, \mathrm{e}^{x\cos\theta}, \quad n = 0, 1, 2, \ldots \tag{1.7.23}$$

The last equality follows since

$$\frac{(2\pi)^2}{\int_{\mathbb{S}} \frac{\mathrm{d}\theta}{p(\theta)}} = \frac{(2\pi)^2}{\int_{\mathbb{S}} \mathrm{d}\theta \mathrm{e}^{2Kr\cos\theta} \int_{\mathbb{S}} \mathrm{d}\theta \mathrm{e}^{-2Kr\cos\theta}} = \frac{1}{I_0^2(2Kr)}. \tag{1.7.24}$$

Using the definition of the Bessel function and the expression for $q(\theta)$, (1.7.5) we can rewrite

$$\frac{I_0(2Kr) + I_2(2Kr)}{2r^2 I_0(2Kr)} = \frac{1}{2r^2} + \frac{I_2(2Kr)}{2r^2 I_0(2Kr)}. \tag{1.7.25}$$

But we also know that (by the self-consistency relation)

$$r = \frac{I_1(2Kr)}{I_0(2Kr)}, \tag{1.7.26}$$

and so (1.7.5) becomes

$$\frac{I_0^2(2Kr)}{2I_1^2(2Kr)} + \frac{I_0(2Kr)I_2(2Kr)}{2(I_1(Kr))^2}, \tag{1.7.27}$$

which is certainly not equal to (1.7.22). Surprisingly, the difference between (1.7.27) and (1.7.22) is numerically very small, a fact that is crucial in Chapter 4 where we will use the term calculated via Itô-calculus as an approximation.

§1.8 Main results of Part II

Results of Chapter 4

In Chapter 4 we consider the Kuramoto model on the hierarchical lattice and make a conjecture on the scaling behaviour of the system at each hierarchical level based on the folklore of renormalization theory. After that we approximate the renormalization scheme and argue that the approximation is good based on the observation that the discrepancy at the first hierarchical level is small. The approximate system can be analyzed exactly, and so we proceed by proving classification criteria for three universality classes in the behaviour of the system, in the hierarchical mean-field limit. The possible universality classes are:

(1) Synchronization is lost at a finite level:
$R^{[k]} > 0$, $0 \le k < k_*$, $R^{[k]} = 0$, $k \ge k_*$ for some $k_* \in \mathbb{N}$.

(2) Synchronization is lost asymptotically:
$R^{[k]} > 0$, $k \in \mathbb{N}_0$, $\lim_{k\to\infty} R^{[k]} = 0$.

(3) Synchronization is not lost asymptotically:
$R^{[k]} > 0$, $k \in \mathbb{N}_0$, $\lim_{k\to\infty} R^{[k]} > 0$.

Here $R^{[k]}$ gives the synchronization in the k-block around the origin. The first main result gives the following criteria:

1.8.1 Theorem. *(Criteria for the universality classes)*

- $\sum_{k\in\mathbb{N}} K_k^{-1} \ge 4 \implies$ *universality class* (1),
- $\sum_{k\in\mathbb{N}} K_k^{-1} \le \frac{1}{\sqrt{2}} \implies$ *universality class* (3),

where K_k is the interaction strength between oscillators at hierarchical distance k.

This result is reminiscent of that in Theorem 1.6.1 without the complication of the sequential dependence on lower levels. The second main result gives bounds on the synchronization levels in different universality classes:

1.8.2 Theorem. *(Bounds for the block synchronization levels)*

- *In universality classes* (2) *and* (3),

$$\tfrac{1}{4}\sigma_k \le R^{[k]} - R^{[\infty]} \le \sqrt{2}\,\sigma_k, \qquad k \in \mathbb{N}_0, \tag{1.8.1}$$

with $\sigma_k = \sum_{\ell>k} K_\ell^{-1}$.

- *In universality class* (1)*, the upper bound in* (1.8.1) *holds for* $k \in \mathbb{N}_0$*, while the lower bound in* (1.8.1) *is replaced by*

$$R^{[k]} - R^{[k_*-1]} \geq \tfrac{1}{4} \sum_{\ell=k+1}^{k_*-1} K_\ell^{-1}, \qquad 0 \leq k \leq k_* - 2. \tag{1.8.2}$$

  The latter implies that

$$k_* \leq \max \left\{ k \in \mathbb{N} \colon \sum_{\ell=1}^{k-1} K_\ell^{-1} < 4 \right\}, \tag{1.8.3}$$

  because $R^{[0]} = 1$ *and* $R^{[k_*-1]} > 0$*.*

The last part of Chapter 4 gives some numerical calculations demonstrating the results above. Chapter 4 is based on [52].

Results of Chapter 5

In Chapter 5 we consider the Kuramoto model on a simpler network, consisting of two communities, and allow the interaction between the communities, L, to be negative. The negative interaction between the communities enriches the model significantly. In particular, the synchronization levels in the two communities can be different. We conjecture that the only possible steady states of the system occur when the phase difference between the average phases of the communities is 0 or π. The nonsymmetric solutions bifurcate from the symmetric solution in both cases. Chapter 5 has three key results. The first is a full classification of the phase diagram of the model, which is summarized in Fig. 1.4 for the case where the phase difference is 0 .

The second result is a characterization of the bifurcation point.

1.8.3 Theorem (Characterization of the bifurcation line). *The existence of non-symmetric solutions requires* $L < 0$*, in which case the bifurcation point* $K^* = K^*(L)$ *is the unique solution to the equation*

$$\sqrt{1 - \frac{2K}{K^2 - L^2}} = V\left((K+L)\sqrt{1 - \frac{2K}{K^2 - L^2}} \right), \tag{1.8.4}$$

and the synchronization level at the bifurcation point is given by

$$r^*(K^*, L) = \sqrt{1 - \frac{2K^*}{K^{*2} - L^2}}. \tag{1.8.5}$$

Here, the function $V(x)$ is defined as

$$V(x) = \frac{\int_{\mathbb{S}} \mathrm{d}\theta \, \cos\theta \, \mathrm{e}^{x\cos\theta}}{\int_{\mathbb{S}} \mathrm{d}\theta \, \mathrm{e}^{x\cos\theta}}, \tag{1.8.6}$$

K is the intra-community interaction strength, and r^* is the synchronization level of the bifurcation point.

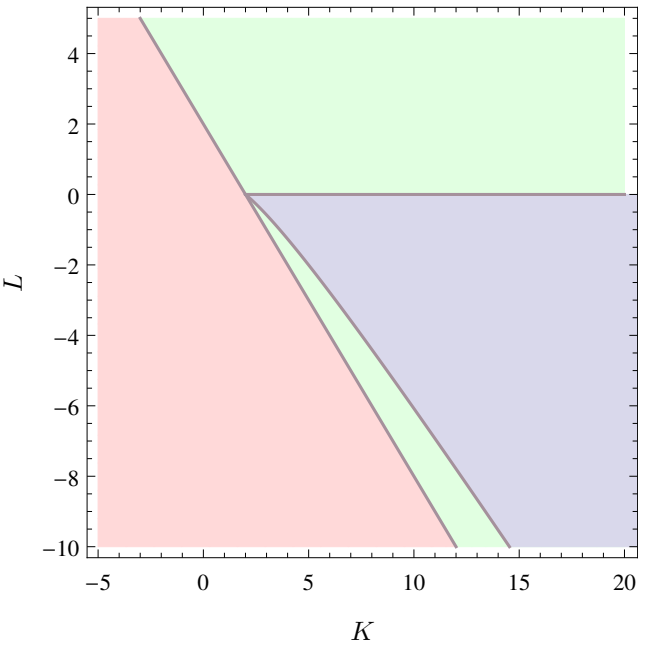

Figure 1.4: In the light red region there is one solution: unsynchronized. In the light green region there are two solutions: unsynchronized and symmetric synchronized. In the light blue region there are three solutions: unsynchronized, symmetric synchronized and non-symmetric synchronized.

The third result consists of a pair of theorems, the first listing properties of the line $r^*(K)$ and the second giving the asymptotics of $L^*(K)$, obtained by fixing K, solving (1.8.4), and letting $K \to \infty$ and $K \downarrow 2$.

1.8.4 Theorem (Properties of $K \mapsto r^*(K)$).

(a) $\lim_{K\downarrow 2} r^*(K) = 0$.

(b) $\lim_{K\to\infty} r^*(K) = 1$.

(c) $r^*(K) \sim \sqrt{\frac{K-2}{2}}$ *as* $K \downarrow 2$.

(d) $1 - r^*(K) \sim \frac{1}{2\sqrt{K}}$ *as* $K \to \infty$.

(e) $\frac{\partial r^*(K)}{\partial K} > 0$ *for all* $K > 2$.

(f) $\frac{\partial^2 r^*(K)}{\partial K^2} < 0$ *for all* $K > 2$.

1.8.5 Theorem (Asymptotic properties of the bifurcation line).

(a) $\lim_{K\to\infty} \frac{\partial L^*(K)}{\partial K} = -1$.

(b) $\lim_{K\downarrow 2} \frac{\partial L^*(K)}{\partial K} = -\frac{1}{2}$.

The model we consider is a special case of the more general model discussed in [120], but we do not rely on a Gaussian approximation. Chapter 5 is based on [93].

Results of Chapter 6

The final chapter of this thesis is an application of the results in Chapter 5 in the field of neuroscience. The results hint at the mechanisms that could be driving a phenomenon observed in some hamsters called *phase splitting*. In experiments [96], [56], [55] hamsters are entrained to a light-dark cycle. In this simulation of night and day, the hamsters are active for a few consecutive hours, once every 24 hours. The hamsters are then switched to a state of constant light. After some time the hamsters exhibit a behavior in which they are active for two periods during the day. How precisely this happens is not know, although many models have been proposed to explain it [117], [98], [65]. In Chapter 6 we propose that the community network structure of the suprachiasmatic nucleus (the body clock) plays a significant role in producing the phase split state. The model in Chapter 5 predicts precisely this phase split state when the interaction between the two communities is negative.

In experiments the phase split state does not seem to be completely stable, as the hamsters switch back to a single active period after some time. Delving deeper into the experiments, we find that the transition to the phase split state can occur in one of two ways. The transition can be smooth, so that the communities change to the phase split state while remaining relatively well synchronized within the communities. The transition can also be quite chaotic, meaning that one or both of the communities become desynchronized before changing to the phase split state. One explanation of this observation could be the nonexistence or existence of nonsymmetric synchronized states found in Chapter 5 that the system might have to pass through before reaching the phase split state. Chapter 6 does not offer new mathematical results and also does not present new experimental findings however, it does offer an interpretation of the mathematical results of Chapter 5 in a specific context and provides data that corroborates this interpretation. The goal of Chapter 6 is to entice experimental researchers to design experiments in order to prove or disprove the predictions made in Chapter 6.

Open Problems

Open problems are numerous. The most challenging is to write down and analyze the true renormalization map for the Kuramoto model on the hierarchical lattice. Another, slightly more realistic, extension would be to include disorder in the hierarchical Kuramoto model and finding an appropriate approximation to the renormalization map with disorder. For the two-community Kuramoto model it would be interesting to analyze the stability properties of the stationary states and to study the dynamics of the system as it moves from one state to the other. Another problem would be to see whether the system bifurcates in the disordered case as well, which we expect to be the case.